ISSN: 2583-9888
DOI: doi.org/10.51219/JAIMLD/keval-babu/501

URF PUBLISHERS
connect with research world

Journal of Artificial Intelligence, Machine Learning and Data Science

https://urfpublishers.com/journal/artificial-intelligence

Vol: 2 & Iss: 4

Research Article

Evaluation of Suspension Characteristics for Battery Electric Vehicle

Keval Babu*

Citation: Babu K. Evaluation of Suspension Characteristics for Battery Electric Vehicle. *J Artif Intell Mach Learn & Data Sci 2024*, 2(4), 2302-2309. DOI: doi.org/10.51219/JAIMLD/keval-babu/501

Received: 03 October, 2024; **Accepted:** 28 October, 2024; **Published:** 30 October, 2024

***Corresponding author:** Keval Babu. Independent Researcher, California, USA

ABSTRACT

This study presents a comprehensive analysis of NTU's Battery Electric Vehicle (BEV) suspension system. The front and rear shock absorbers' inclination angles and their impact on spring rates, wheel rates, ride rates and suspension frequencies were meticulously calculated, revealing a slightly softer ride due to lower-than-typical frequencies. The roll rate analysis highlighted the importance of weight transfer dynamics in vehicle handling, with a higher rear roll rate indicating faster weight transfer to the rear axle. The roll gradient, confirming minimal body roll, enhances stability and aligns with the desired handling performance. The damping coefficient and ratio calculations, referenced from OEM manuals, ensure optimal vibration dampening and ride quality. Adjustments to shock absorber heights were made to achieve the desired center of gravity. This research underscores the critical role of precise suspension design and optimization in achieving a balanced and responsive driving experience for NTU's BEV.

Keywords: BEV, EV, Suspension system, Wishbone, SLA. C.G., Roll Rate, Ride Height, MR, Dampening, Spring Rate

1. Introduction

The world continues to grapple with the persistent challenge of global warming, compounded by environmental pollution which poses a significant threat to human health. A key contributor to this problem is the exhaust gases emitted by conventional internal combustion engine vehicles. Over the years, the global vehicle count is projected to reach approximately 1.8 billion and the continuous rise in oil prices underscores the urgency of adopting sustainable and alternative mobility technologies.

Plug-in and hybrid vehicles are promising alternatives that hold substantial potential for mitigating these issues. This project, initiated by Nanyang Technological University (NTU), Singapore, focuses on the research and development of a student-designed electric car. Electric vehicles (EVs) are gaining traction worldwide due to their eco-friendly nature and zero emissions. NTU's Battery Electric Vehicle (BEV) is an urban concept car that leverages Singapore's compact geographical area, making it an ideal location for the adoption of electric cars.

The continuous escalation of oil prices and the intensifying impact of global warming have necessitated the adoption of alternative mobility technologies. Electric vehicles (EVs) present a compelling alternative to conventional internal combustion engine vehicles.

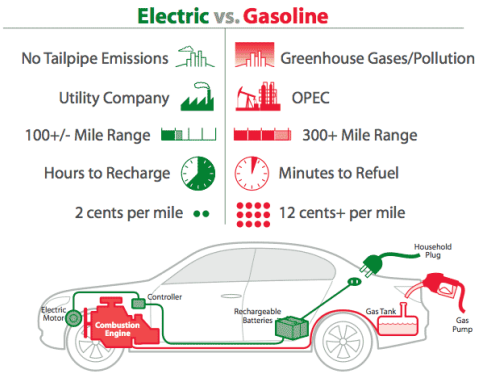

Figure 1: Electric v/s Gasoline. (Circuits-today, 2010).

Atmospheric pollution from exhaust gases emitted by internal combustion engines, coupled with the constant rise in oil prices, has paved the way for the adoption of electric cars globally. Electric vehicles offer significant advantages over conventional internal combustion engine vehicles, including lower operating and maintenance costs, as well as higher efficiency as shown in **(Figure 1**). Electric cars centralize pollution sources to power stations that generate electricity, whereas conventional cars distribute pollution, making them less efficient. Although the limited range of electric cars has been a discouraging factor, continuous advancements are being made to enhance their range. Numerous automakers, such as Honda, Toyota, Mercedes-Benz, BMW and Tesla, have already commenced manufacturing electric street and sports cars as shown in **(Figure 2)**.

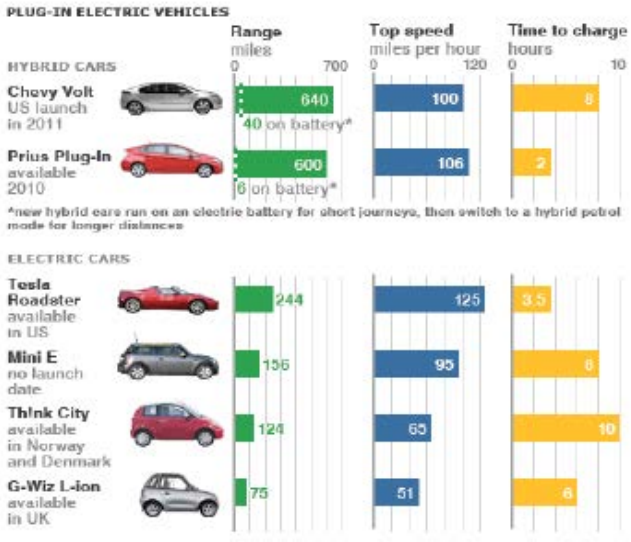

Figure 2: Different plug-in electric cars. (Becker, 2009).

An electric car is a vehicle powered by an electric motor, utilizing electrical energy stored in devices such as batteries or capacitors. A plug-in electric car is recharged using an external electricity source.

Electric vehicles, including hybrid and plug-in electric cars, are poised to play a crucial role in the future mobility landscape, particularly in Singapore and globally. This project aims to challenge students to design and stimulate their creativity, fostering innovative ideas and solutions to bring NTU's first plug-in electric car to life. The concept of the Battery Electric Vehicle (BEV) revolves around generating clean energy from lithium-ion battery packs. The electrical power is directed to the motor through a controller, which in turn drives the rear differential.

This paper includes detailed explanations on evaluation of suspension characteristics for BEV's suspension system.

1.1. Suspension system overview

The suspension system is a three-dimensional four-bar linkage that includes shock absorbers, springs and linkages, which connect the vehicle chassis to its wheels, allowing for relative motion between the two. The suspension system fulfills three primary roles:

- **Comfort:** It provides vertical compliance, enabling the wheels to follow the road surface, while isolating the chassis from road roughness to enhance passenger comfort.
- **Safety:** It responds to control forces produced by the tires, including longitudinal and lateral forces, as well as braking and driving torques. This ensures the protection of passengers, luggage, other mechanical and electrical systems and the vehicle itself.
- **Handling:** It maintains tire contact with the road with minimal load variations and resists chassis roll. Keeping the wheels in contact with the road surface is crucial, as all road or ground forces acting on the vehicle are transmitted through the tire contact patches.

1.2. Double wishbone suspension system

NTU's Battery Electric Vehicle (BEV) features a double wishbone or short-long arm (SLA) suspension system at both the front and rear wheels. This system includes two unequal-length "A" or "wishbone" shaped control arms that are not parallel. These arms connect to the chassis and sub-frame at one end and the steering knuckle at the other. The upper arms are shorter than the lower ones and are mounted on the chassis, which helps maintain a constant wheel track. Shock absorbers are attached to the lower wishbone and chassis to manage the vehicle's vertical movement. The double wishbone suspension is an independent design that allows for the independent movement of all four wheels, thereby eliminating wheel wobbling as illustrated in **(Figure 3)**.

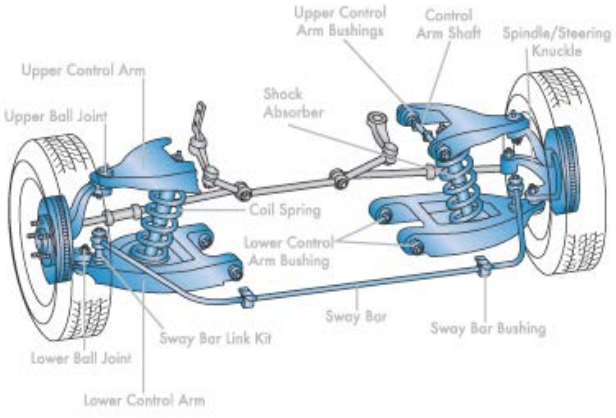

Figure 3: Double wish-bone suspension system. (Automotive artistry, 2014).

1.3. Advantages of SLA suspension system

- **Versatility:** Allows engineers to precisely control wheel motion throughout suspension travel, managing parameters such as camber angle, caster angle, toe pattern, roll center height, scrub radius and scuff.
- **Reduced camber angle gain:** Minimizes changes in track width.
- **Enhanced handling and safety:** Improves handling, driving safety and ride characteristics.
- **Lateral Stiffness:** Provides good lateral stiffness to the vehicle.

1.4. Disadvantages of SLA suspension system:

- **Complexity and cost:** Requires more components, increasing manufacturing costs and space requirements.
- **Installation requirements:** Necessitates a front and rear sub-frame, raising assembly costs, complexity and vehicle weight.

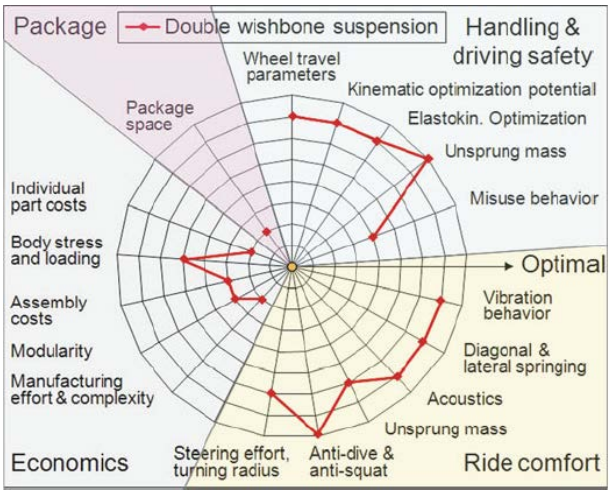

Figure 4: Performance profile-double wishbone suspension system. (A-Z Chassis Handbook, 2011).

The different components of a double wishbone suspension and their roles are as follows:

- **Spring & shock absorber:** Together, they support the weight of the vehicle and enable the control arms and wheels to move up and down. The primary function of the shock absorber is to dampen the body and wheel vibrations caused by uneven roads, while the coil spring cushions these vibrations to provide a comfortable ride. Without the shock absorber, the vehicle would continue to bounce after encountering an uneven road surface.
- **Anti-roll or stabilizer bar:** This component limits the vehicle's body roll during cornering, maintaining constant wheel contact with the road. It connects the lower control arms on both sides of the vehicle through bar links and bushings, reducing excessive body lean or roll by resisting the centrifugal forces experienced during cornering.
- **Mechanism:** This specifies the kinematics of pivot points during lateral and vertical movement, controlling the suspension geometry. The mechanism includes various other components such as:
- **Control arms:** These define the wheel kinematics relative to the chassis. The outer end of the control arm contains a ball joint linked to the steering knuckle, while the inner end consists of a rubber bushing as shown in **(Figure 5)**.

Figure 5: Upper & lower control arms.

Steering knuckle: As shown in **(Figure 6)**, this component accommodates the installation of wheels, braking and steering elements. It features three pivot points that connect to the upper and lower control arms and the steering rod. When the steering is turned, it rotates the knuckle, which subsequently turns the wheel assembly.

Figure 6: Upper & lower control arms.

- **Ball Joints:** These components link the steering knuckle with the control arms, allowing freedom of movement in two translational directions and one rotational direction as illustrated in **(Figure 7)**. The ball joints in the control arms have a spring mounted on them, making them load carriers.

Figure 7: Ball joint. (Melior, Inc. 2004).

- **Bushings:** These supplementary units absorb and isolate vibrations and noise, enhancing the wear resistance of components. Control arm bushings comprise rubber sandwiched between a metal inner sleeve and a metal outer sleeve. The inner sleeve remains stationary, while the outer sleeve moves with the control arm as displayed in figure 8. Bushings are also used in anti-roll bars, shock absorbers and strut rods.

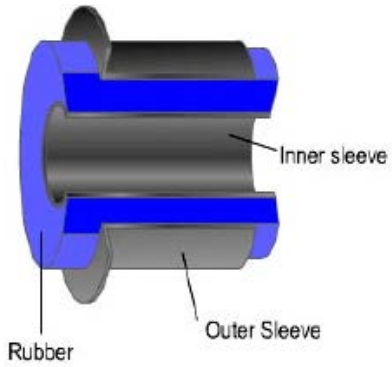

Figure 8: Bushing. (Melior, Inc. 2004).

- **Strut rods:** Strut rods prevent the lower control arm from moving fore and aft, providing stability. They are connected to the frame and bolted to the outer end of the lower control arms. The installation of strut rods typically depends on the drive configuration of the vehicle, whether it is front-wheel drive (FWD) or rear-wheel drive (RWD). In NTU's Battery Electric Vehicle (BEV), strut rods are installed at the rear since it is a RWD car.

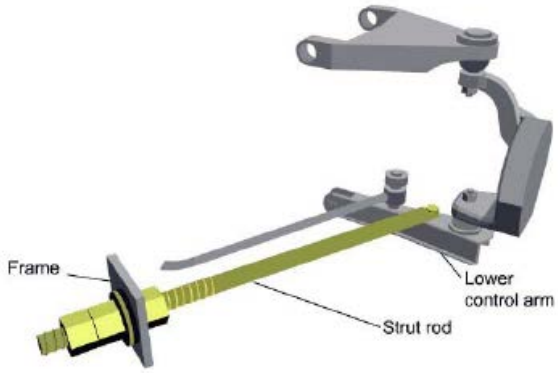

Figure 9: Strut rod. (Melior, Inc. 2004).

1.5. Suspension characteristics

The suspension characteristics and their influence on the handling and performance of the BEV are thoroughly examined. Each of the nine suspension characteristics were evaluated and optimized in detail.

(1) Motion Ratio

The motion ratio, defined as the ratio of shock absorber displacement to wheel displacement, is crucial in suspension design. Designers typically aim to maintain a motion ratio (MR > 0.6) to prevent excessive forces at the tire. This ratio represents the lever arm effect of the control arm on the shock absorber.

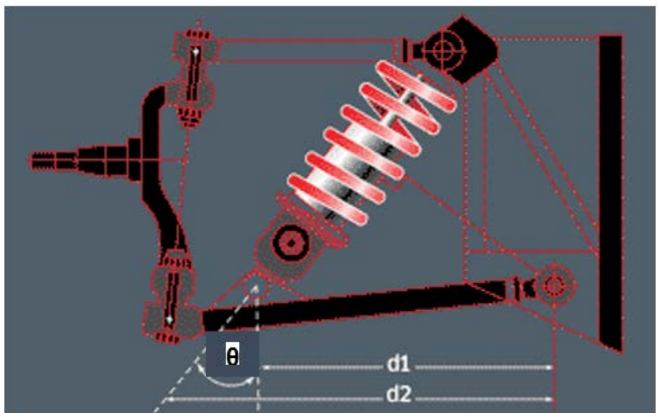

Figure 10: Motion ratio of SLA. (Eibach, 2013).

$$MR = \frac{d_1}{d_2} \ (1)$$

Where, d_1: Distance from shock absorber centerline to control arm inner pivot center

d_2: Distance from outer ball joint to control arm inner pivot center

θ: Shock absorber angle from vertical

Using equation 1, the motion ratios of the front and rear suspensions were calculated by measuring the distances d_1 and d_2, which were 0.73 and 0.7, respectively. These motion ratio values exceed the desired MR, aligning with the design intent. Notably, the shock absorbers are mounted to their respective lower control arms on either side, rather than being directly attached to the wheels.

(2) Spring Rate

Spring rate measures the unit deformation for an applied mass on the spring and represents the spring's stiffness in kg/mm. The front and rear spring rates were determined to be 9.12 kg/mm and 9.15 kg/mm, respectively, calculated using equation 2.

$$k = \frac{G\ d^4}{64\ i\ r_m^3} \ (2)$$

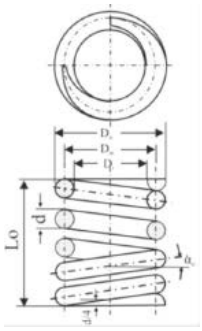

Figure 11: Spring. (P. Aisopoulos, 2011).

Where, G: shear modulus of spring
d: wire diameter of the spring
i: number of active coils
r_m: average radius of coils of the spring
k: spring rate of the spring

Since the shock absorbers are mounted at an angle from the vertical, the equivalent spring rates of the springs were calculated using equation 3.

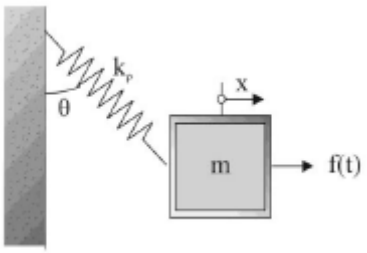

Figure 12: Inclined mass-spring model. (P. Aisopoulos, 2011)

$$k_{eq} = k(\sin\theta)^2 \ (3)$$

Where,

k_{eq}: Equivalent spring rate in kg/mm
k: spring rate in kg/mm
θ: Shock absorber angle from vertical

The angles of inclination for the front and rear shock absorbers were 20.4° and 18.8°, respectively. Consequently, the equivalent spring rates of the front and rear suspension springs were determined to be 8.01 kg/mm and 8.2 kg/mm, respectively.

(3) Wheel Rate

The wheel rate represents the actual rate of a spring acting at the tire contact patch. Given that the shock absorbers are mounted to the lower control arms at an angle, an angle correction factor (ACF) was applied to account for the reduced motion of the shock absorbers. The wheel rates at the front and rear wheels were determined using equation 4.

$$k_w = k_{eq}\ MR^2(ACF)\ where\ ACF = cos\,\theta \ (4)$$

Where, keq: Equivalent spring rate in kg/mm

kw: wheel rate in kg/mm

ACF: Angle correction factor

The wheel rates of the front and rear wheels were determined to be 4.01 kg/mm and 3.72 kg/mm, respectively.

(4) Ride Rate

The suspension system comprises sprung and un-sprung masses, as illustrated in figure 13. The sprung mass includes all non-suspension components (e.g., chassis, engine, differential system, passengers and cargo-luggage) as well as half of the mass of the shock absorber, anti-roll bar and control arms. This mass is supported by the suspension components shown in the figure. Conversely, the un-sprung mass consists of all suspension components located outboard of the upper and lower ball joints (e.g., spindle, wheel, knuckle, brakes) along with half of the mass of the shock absorber, anti-roll bar and control arms. The suspension spring and damper are connected in parallel, isolating the sprung and un-sprung masses. The tire functions as a spring between the road and the un-sprung mass.

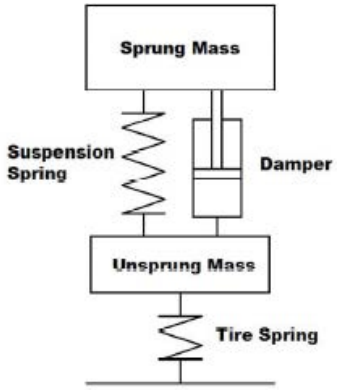

Figure 13: Quarter car model. (Riley Q, 1999).

The effective stiffness of the suspension and tire springs in series is referred to as the ride rate. The ride rates for the front and rear suspensions were calculated as 2.67 kg/mm and 2.55 kg/mm, respectively, using equation 5.

$$k_{eff} = \frac{(k_{eq} k_w)}{(k_{eq} + k_w)} \quad (5)$$

Where, $k_{eq:}$ Equivalent spring rate in kg/mm $k_{w:}$ wheel rate in kg/mm

k_{eff}: Effective spring rate in kg/mm

(5) Suspension Frequency

Suspension frequency is the measure of how many oscillations or "cycles" the suspension undergoes over a specified time period when a load is applied to the vehicle. This frequency was calculated using equation 6.

$$SF = 3.13 \sqrt{\frac{k_w}{m_s}} \quad (6)$$

Where, SF: suspension frequency in Hz

m_s: sprung mass in kg

K_w: wheel rate in kg/mm

The initial front and rear suspension frequencies were determined to be 0.35 Hz and 0.3 Hz, respectively. Typical road cars aim for suspension frequencies between 0.4 and 0.8 Hz to ensure a comfortable ride. The front and rear ride frequencies of NTU's BEV, however, were found to fall outside the traditional range for passenger cars, resulting in a ride that is slightly softer than desired. Achieving these frequencies can be challenging in vehicles with limited suspension travel.

1.6. Two factors contribute to this discrepancy

The control arm geometry was originally designed for the Honda S2000, fixing the motion ratio of the suspension and the mounting angle of the shock absorbers, making these parameters non-adjustable for suspension frequency.

The corner weights and shock absorbers of NTU's BEV differ from those of the Honda S2000. While the spring rate of the coil-over spring is higher than that of the original Honda S2000, the desired suspension frequency can be achieved by adjusting the length of the coil spring once the final corner weights are known.

Lower suspension frequencies result in a softer suspension, providing more mechanical grip but leading to transient response. Most passenger cars have lower suspension frequencies. In contrast, higher suspension frequencies reduce suspension travel and allow for a lower ride height, which in turn lowers the center of gravity and improves stability. High suspension frequencies are typically used in race or sports cars.

Ride frequencies generally differ between the front and rear axles. Matt Giaraffa's theory for passenger cars prioritizes comfort over performance by aiming for lower damping ratios and minimal pitch over bumps. According to this theory, if the front ride frequency is higher than the rear, the resulting phase difference can cause pitching of the car body. The out-of-phase motion between the front and rear vertical movements, caused by the time delay between when the front and rear wheels encounter a bump, is accentuated by the frequency difference.

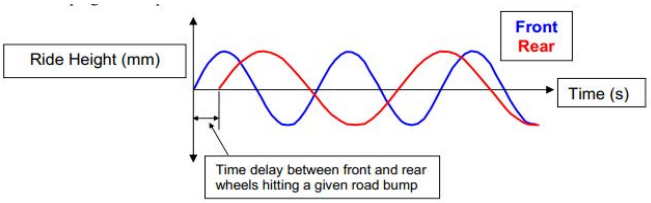

Figure 14: Out-of-phase. (M.Giaraffa, 2013).

According to the theory, the difference between the front and rear ride frequencies should be between 10-20%. Therefore, it is suggested to reduce the pitch by aligning the rear ride frequency with the front. This concept of minimizing induced body pitch is known as "flat ride."

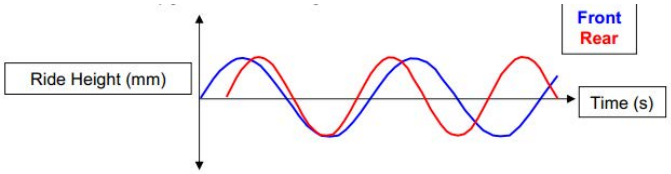

Figure 15: Flattening notion. (M.Giaraffa, 2013).

The 13.3% difference between the front and rear ride frequencies of NTU's BEV meets the traditional design criteria.

(6) Roll Rate

Roll rate refers to the rate at which a vehicle's sprung mass rolls about its roll axis due to lateral acceleration, expressed as torque per degree of roll. The front and rear roll rates of a vehicle typically differ, playing a crucial role in determining the vehicle's turning capability during transient and steady-state handling. Several factors influence a vehicle's roll rate, including

the center of gravity (C.G.), anti-roll bar stiffness, wheel rates, roll center height, track width and sprung mass.

The roll rate's physical significance lies in how quickly and what percentage of weight is transferred from one axle to the other through the vehicle chassis. A higher roll rate on an axle results in faster and greater weight transfer on that particular axle and vice-versa. The roll rates of the front and rear axles were calculated using equations 7 and 8.

$$K_{\varphi F} = \frac{\pi\, t_f^2 K_{LF} K_{RF}}{180(K_{I,F} + K_{RF})} \quad (7)$$

$$K_{\varphi R} = \frac{\pi t_r^2 K_{LR} K_{RR}}{180(K_{I,R} + K_{RR})} \quad (8)$$

Where, $K_{\varphi F}$= Front roll rate in Nm/deg roll
$K_{\varphi R}$= Rear roll rate in Nm/deg roll
t_f= front track width in m
t_r = rear track width in m
K_{LF} = left front wheel rate in N/m
K_{RF} = right front wheel rate in N/m
K_{LR} = left rear wheel rate in N/m
K_{RR} = right rear wheel rate in N/m

The front and rear roll rates of the BEV were calculated to be 762.17 Nm/deg and 764.64 Nm/deg, respectively. The rear roll rate being slightly higher than the front indicates that weight transfer to the rear axle could occur more quickly and with a higher percentage.

(7) Roll Gradient

The roll gradient is defined as the rate of change of the vehicle's roll angle with steady-state lateral acceleration values, expressed in g's. It indicates the extent to which the vehicle rolls per unit of lateral acceleration. A lower roll gradient results in less body roll per g of lateral acceleration. While a vehicle with a lower roll gradient responds more quickly in transient conditions, it may lose some mechanical grip when cornering. Roll gradient influences a vehicle's handling performance and for compact cars, the desired roll gradient should be ≤ 5 deg/g. A higher roll gradient would lead to excessive body roll and an uncomfortable ride. The roll gradient was calculated using equation 9.

$$\frac{\varphi_r}{A_y} = \frac{-WH}{(K_{\varphi F} + K_{\varphi R})} \quad (9)$$

Where, $\frac{\varphi_r}{A_y}$= Rolls gradient in deg/g
W= weight of the car
H = distance between roll axis and C.G
$K_{\varphi F}$= Front roll rate in Nm/deg roll
$K_{\varphi R}$= Rear roll rate in Nm/deg roll

The BEV exhibits a roll gradient of 2.26 deg/g, meaning it rolls 2.26° for every g of lateral acceleration. This roll gradient value falls within the desired range.

(8) Suspension Damping

Shock absorbers are used to dampen vibrations. The maximum damping force depends on the weight of the components being dampened, the spring rate, the ratio of wheel displacement to damper stroke and the angle of the damper relative to the vehicle's vertical axis.

Figure 16: Car roll. (Raw-autos, 2014)

The damping coefficient values were referenced from the OEM manual provided with the Tein advanced street flex shock absorbers. The damping coefficients for the front and rear shock absorbers were 1733.33 N-s/m and 2083.33 N-s/m, respectively. The damping coefficient graph from the OEM manual is re-generated below.

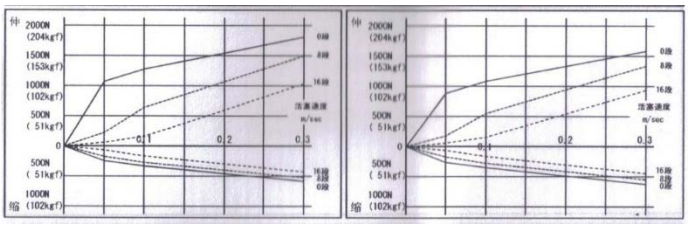

Figure 17: Damping curves (Front & Rear). (Tein USA, 2013)

The damping ratio, a dimensionless quantity, describes how oscillations in a system decay after a disturbance. Shock absorbers dampen road surface vibrations through the un-sprung mass and isolate the chassis. The damping ratio was calculated using equation 10, as all other parameters were known.

$$\zeta = \frac{k}{\sqrt{k_w m_s}} \quad (10)$$

where, ζ: damping ratio
k_w: wheel rate in kg/mm
m_s: sprung mass in kg
k: damping coefficient in N-s/m

The damping ratios for the front and rear suspensions of the BEV were calculated to be 0.28 and 0.31, respectively. For a comfortable ride, the damping ratio should fall within the range of 0.2-0.4. This design criterion ensures moderate vertical acceleration at low frequencies and high attenuation at high frequencies, as illustrated in figure 18.

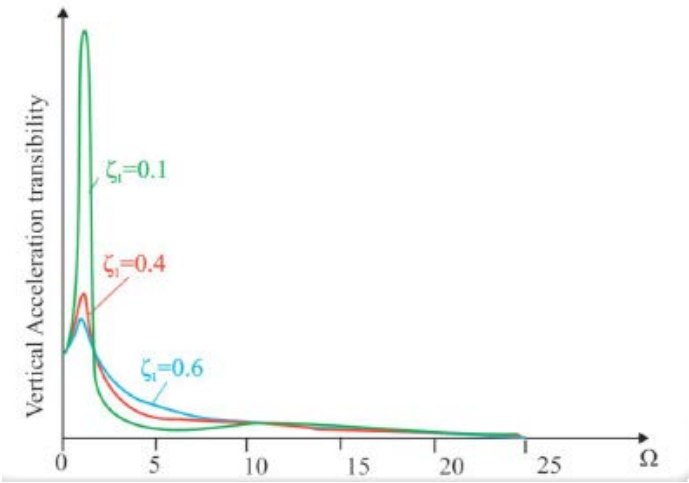

Figure 18: Transibility curve. (P. Aisopoulos, 2011).

The OEM's manual indicated a piston velocity of 0.3 m/s within the damper. Using this information and the known parameter values, the average damper force F_m was calculated using equation 11.

$$F_m = 2V_D\zeta i^2\sqrt{k_w m_s} \quad (11)$$

Where, F_m: Average damping force in N i: 1/Motion ratio
V_D: Piston velocity in damper in m/s

After determining the average damping force of the front and rear shock absorbers, the damping force experienced during the compression and rebound stages of all four shock absorbers was calculated using equations 12 and 13. The rebound to compressive force ratio for passenger cars is typically estimated to be 4.

$$F_c = F_m\left(\frac{2}{1+q}\right) \quad (12)\ F_r = F_m\left(\frac{2q}{1+q}\right) \quad (13)$$

Where, F_t: Rebound damping force in N
F_c: Compressive damping force in N
q: ratio of rebound to compressive force
F_m: Average damping force in N

The damping force calculations value are tabulated in the table 1 below.

Table 1: Damping forces.

Damping force (N)	Front shock absorber	Rear shock absorber
F_m	975.98	1314.06
F_c	390.39	525.62
F_t	1561.57	2102.49

(9) Ride Height Adjustment

Vehicle ride height, essentially the ground clearance, should be minimized for several reasons:

1. Lower ride height results in a lower center of gravity, enhancing handling characteristics and vehicle stability.
2. It reduces aerodynamic drag and increases aerodynamic down-force.

The desired center of gravity (C.G) for the BEV was approximately 370 mm from the ground. To achieve this, adjustments to the shock absorber height were necessary to modify the ground clearance. The maximum and minimum adjustable heights of the shock absorbers were evaluated and the range of height adjustment was determined by finding the difference between these maximum and minimum heights.

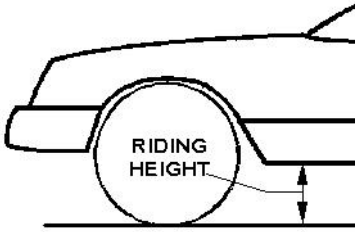

Figure 19: Ride height. (F&F tire world, 2013).

The installation height of the shock absorbers was determined by summing the minimum height and 40% of the adjustment range. The installation shock absorber heights for the front and rear were 516.7 mm and 509.3 mm, respectively.

$$Installation\ height = min.height + 0.4(range) \quad (14)$$

The laden and un-laden heights of the shock absorbers were then determined. Un-laden height corresponds to the height of the shock absorbers when the car is empty (i.e., no passengers on board), whereas laden height refers to the height when the car is fully loaded with passengers. Equations 15 and 16 were used to calculate these heights.

$$Unladen\ height = installation\ height - \frac{unladen\ mass}{k_{eqf}} \quad (15)$$

$$Laden\ height = installation\ height - \frac{laden\ mass}{k_{eqr}} \quad (16)$$

Where, k_{eqf} : equivalent front spring rate in kg/mm
k_{eqr}: equivalent rear spring rate in kg/mm

The laden and un-laden heights for the front shock absorbers were determined to be 474.86 mm and 485.5 mm, respectively. Similarly, the laden and un-laden heights for the rear shock absorbers were found to be 459.35 mm and 472.02 mm, respectively.

2. Conclusion

The comprehensive analysis of NTU's BEV suspension system reveals several critical insights and findings. The initial assessment of the front and rear spring rates, along with the calculation of equivalent spring rates, highlights the importance of considering shock absorber inclination angles. Subsequent calculations of wheel rates, ride rates and suspension frequencies underline the need for precise adjustments to achieve optimal performance characteristics. While the front and rear ride frequencies fall slightly outside the traditional range, the design considerations provide a foundation for achieving desired suspension performance.

Further evaluation of roll rates emphasizes the significance of weight transfer dynamics and the impact on vehicle handling during transient and steady-state conditions. The roll gradient analysis confirms the design's alignment with desired handling performance, ensuring minimal body roll and enhanced stability. The damping ratio calculations and the determination of laden and un-laden shock absorber heights contribute to achieving the desired center of gravity and overall ride quality.

Ultimately, this study underscores the critical role of meticulous suspension design and optimization in enhancing vehicle performance, stability and comfort. By addressing key

parameters such as spring rates, damping coefficients, roll rates and ride heights, NTU's BEV aims to deliver a well-balanced and responsive driving experience.

3. References

1. http://www.worksevo.com/Spring_Rates_1.pdf
2. http://www.autoshop101.com/
3. Becker B. "Electric vehicles in the United States, A new model with forecast to 2030," Center for Entrepreneurship & Technology, University of California, Berkeley, Technical Brief, 2009.
4. HeiBing B. M. E. "Chassis Handbook Fundamentals, Driving dynamics, Components, Mechatronics, Perspectives," 1st ed., Berlin, Germany: Vieweg and Tuebner, 2011.
5. Sandalow DB. "Plug-In Electric Vehicles: What Role for Washington?" 1st ed., The Brookings Institution, 2009.
6. Dixon JC. "Tires, Suspension and Handling," 2nd ed., SAE, Arnold, 1996.
7. Dixon JC. "Suspension Geometry," John Wiley & Sons Ltd., 2009.
8. Aisopoulos PJ. "Suspension System," Department of Vehicles, Alexander Technological Educational Institute of Thessaloniki Greece.
9. Hathaway R. "Vehicle structural design," 2008.
10. http://eibach.com/america/en/motorsport/products/suspension-worksheet.
11. Beer Jr F, Johnston ER, DeWolf J and Mazurek D. "Mechanics of materials," 6th ed., 4th ed., SAE International, 2009.
12. http://www.optimumg.com/technical/technical-papers/.
13. Gilles T. "Automotive Chassis Brake, Suspension and Steering," California: Thomson Delmar Learning, 2005.
14. Gillespie TD. "Fundamentals of vehicle dynamics," 1992.
15. Hartley J. "Automobile Steering and Suspension," Newnes Technical Books, Haynes Publishing, 1985.
16. Howard G, Bastow D and Whitehead JP. "Car Suspension and Handling," 2004.
17. http://www.ignou.ac.in/upload/Unit-6-61.pdf.
18. http://www.stoptech.com/docs/media-center-documents/the-physics-of-brakingsystems?sfvrsn=42.
19. Jurgen RK. "Electronic Steering and Suspension System," SAE International, Warrendale, United State of America, 1999.
20. Jurgen RK. "Electric and Hybrid-Electric Vehicles Engines and Powertrains," SAE International, Warrendale, United State of America, 2011.
21. Malen DE. "Fundamentals of Automobile Body Structure Design," SAE International, 2011.
22. Milliken WF, Milliken DL. "Race Car Vehicle Dynamics," Warrendale, PA: Society of Automotive Engineers, 1995.
23. Mitchell WJ, Borroni-Bird C and Burns LD. "Reinventing the automobile, personal urban mobility for the 21st century," The MIT Press, 2012.
24. http://www.fkm.utm.my/~arahim/daimlerchrysler-gritt.pdf.
25. Reynolds J. "Brakes," Alabama: Automotive Mechanics, 1986.
26. https://doi.org/10.1007/978-0-387-74244-7.
27. http://www.rqriley.com/suspensn.htm.
28. Srinivasan S. "Automotive Mechanics," 2nd ed., Tata McGraw Hill Education Pvt. Ltd., 2003.
29. Staniforth A. "Competition Car Suspension Design, Construction, Tuning," 1999.
30. Steering and Suspension Systems Study Guide, Melior, Inc., 2004.
31. The Mark Ortiz Automotive, "CHASSIS NEWSLETTER," 2002.
32. Harbin W. "Suspension and chassis glossary," Technical Director at BND TechSource, 2013.
33. http://yospeed.com/wheel-alignment-explained-camber-caster-toe/.
34. Cai Z, Chan S, Tang X and Xin J. "The Process of Vehicle Dynamics Development," 2012.